

Thickness-dependent coercive mechanisms in exchange-biased bilayers

C. Leighton,¹ M. R. Fitzsimmons,² A. Hoffmann,³ J. Dura,⁴ C. F. Majkrzak,⁴ M. S. Lund,¹ and Ivan K. Schuller⁵

¹*Department of Chemical Engineering and Materials Science, University of Minnesota, Minneapolis, Minnesota 55455*

²*Los Alamos National Laboratory, Los Alamos, New Mexico 87545*

³*Argonne National Laboratory, Materials Science Division, 9700 S. Cass Avenue, Argonne, Illinois 60439*

⁴*National Institute of Standards and Technology, Gaithersburg, Maryland 20899*

⁵*Physics Department, University of California at San Diego, La Jolla, California 92093-0319*

(Received 30 July 2001; published 4 January 2002)

We present an investigation of the effect of ferromagnetic layer thickness on the exchange bias and coercivity enhancement in antiferromagnet/ferromagnet bilayers. At low temperatures both the exchange bias and coercivity closely follow an inverse thickness relationship, contrary to several recent theoretical predictions. Furthermore, the temperature dependence of the coercivity as a function of the ferromagnet thickness provides clear evidence for the existence of two distinct regimes. These regimes were probed with conventional magnetometry, anisotropic magnetoresistance, and polarized neutron reflectometry. At low thickness the coercivity exhibits a monotonic temperature dependence, whereas at higher thickness a broad maximum occurs in the vicinity of the Néel temperature. These regimes are delineated by a particular ratio of the ferromagnet to antiferromagnet thickness. We propose that the ratio of the anisotropy energies in the two layers determines whether the coercivity is dominated by the ferromagnetic layer itself or the interaction of the ferromagnetic layer with the antiferromagnet.

DOI: 10.1103/PhysRevB.65.064403

PACS number(s): 75.70.Cn, 75.30.Gw

INTRODUCTION

As a result of the lack of understanding of the basic mechanism for unidirectional anisotropy at antiferromagnet/ferromagnet (AF/F) interfaces, interest in exchange-biased systems continues.¹ This continued interest is no doubt also stimulated by the fact that the exchange biasing phenomenon is being used in devices in the magnetic recording industry to pin the magnetization of ferromagnetic layers.^{1,2} Recent years have seen a shift in fundamental research toward understanding the mechanism of magnetization reversal, which determines the coercivity. The interest in coercive mechanisms was stimulated by several factors including the realization that the reversal mechanisms are intrinsically asymmetric^{3–10} and that the phenomenology associated with the enhanced coercivity (H_C , the zero-moment half-width of the hysteresis loop) provides important information on the fundamental origin of the exchange bias (H_E , the loop shift) and the coupling mechanism between the AF and F layers.¹¹

Several explanations for the coercivity enhancement have been advanced, based on experimental^{12,13} and theoretical^{11,14,15} investigations. They include perpendicular coupling between the layers,¹¹ “Malozemoff-type” domains which pin ferromagnetic domain walls,¹⁴ interfacial magnetic frustration,¹² enhanced higher order anisotropies,¹³ and irreversible (or reversible) changes in AF spin structure on reversal of the F layer.¹⁵ What has become clear due to this recent work is that the reversal of the F layer is not simply due to coherent rotation on both sides of the loop and that models which do not incorporate a realistic description of the reversal mechanism cannot possibly capture the essential physics. Two of the most recent investigations which have made attempts to realistically model the coercive mechanisms are those of Stiles and McMichael¹⁵ and Li and Zhang.¹⁴ Li and Zhang¹⁴ modeled the coercivity enhance-

ment as being due to effective pinning of F layer domain walls by AF domains perpendicular to the interface.¹⁶ On the other hand, Stiles and McMichael¹⁵ have presented a very comprehensive picture of coercive behavior in polycrystalline AF/F systems which highlights the importance of irreversible changes in AF spin structure during reversal of the ferromagnet. They find that there are two regimes of behavior. In one, the losses are primarily in the F layer and stem from inhomogeneities in the coupling to the AF layer, while in the other irreversible changes in the AF spin structure lead to losses which mainly arise in the antiferromagnet itself. Note that by “losses” we mean energy losses due to irreversible changes in spin structure, e.g., due to domain wall motion, for instance. A simple way to visualize such a scenario is that large stable AF grains reverse in unison with the F layer, while small, unstable, AF grains are subject to irreversible losses due to the weaker effective coupling between the individual grain and ferromagnet. This model can be formulated in terms of “rotatable” and “nonrotatable” components in the anisotropy.^{15,17}

A common feature in both models is that the F layer thickness dependence of the coercivity is very sensitive to the coercive mechanism at work. Traditionally, it has often been assumed that both the exchange bias and coercivity vary as $H \propto 1/t_F$, where t_F is the thickness of the F layer.¹ This can be rationalized as a simple consequence of the fact that the exchange bias effect is an interfacial one. However, Dimitrov and co-workers argued on general grounds^{18,19} that the perpendicular domain model for coercivity enhancement via F domain wall pinning should lead to

$$H_C \propto \frac{1}{t_F^n}, \quad (1)$$

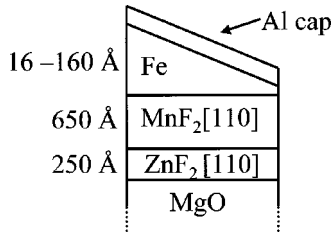


FIG. 1. Schematic of the sample structure. Details of the film deposition are given in the text.

where $n = 1.5$. This prediction was experimentally verified by Dimitrov *et al.*,¹⁸ Zhang *et al.*,¹⁹ and Zhuo *et al.*²⁰ Further analysis of the micromagnetic simulations based on this model showed that the exponent n is dependent on grain sizes and the thickness regime for the ferromagnetic layer, in all cases being greater than 1. The model of Stiles and McMichael¹⁵ also makes clear predictions regarding the F layer thickness dependence of the coercivity enhancement. Specifically, it was shown that at low temperatures (when the losses are primarily in the F layer) $n = 2$, while at high temperatures (when the losses are primarily in the AF layer) $n = 1$ is recovered. It is also worth noting that the model of Stiles and McMichael¹⁵ also predicts that the thickness dependence of the *exchange bias* should exhibit small departures from $1/t_F$ so that

$$H_E \propto \frac{1}{t_F^m}, \quad (2)$$

where the exponent m is not necessarily 1. Given this theoretical evidence that the thickness dependence of the coercivity enhancement can shed light on the fundamental mechanisms, it is clear that a comprehensive experimental investigation is required. Despite the many investigations of the coercivity enhancement, very few authors have performed systematic investigations of the F layer thickness dependence (i.e., a determination of n) in well-characterized systems.

To systematically investigate the F layer thickness dependence of the coercivity enhancement, we have fabricated wedges of variable thickness of Fe on MnF₂ antiferromagnetic layers. Note that the AF layers are epitaxial, but twinned (a full description of the structure is given below), while the F layers are polycrystalline. A schematic of the sample structure is shown in Fig. 1. This materials system was chosen as it has proved to be a model system for exchange bias studies due to the well-understood nature of the antiferromagnetism and controllable epitaxy. In this system we have previously studied the effects of interface disorder,²¹ coercivity enhancements,¹² and asymmetric magnetization reversals,^{4–7} providing a large body of experimental knowledge of the exchange bias and surrounding phenomenology.

EXPERIMENTAL CONSIDERATIONS

The samples were deposited by sequential electron beam evaporation as detailed in previous publications.^{4–7,12} Briefly, the fluoride layers are deposited from pressed powder targets

at a rate of 1 Å s^{-1} onto MgO [100] substrates while the metal overlayers are deposited from elemental targets at a rate of 0.8 Å s^{-1} . The substrates (which are chemically cleaned prior to loading into the vacuum system) are annealed *in vacuo* at 500°C for 1 h immediately prior to deposition. The base pressure of the system is in the low- 10^{-8} -Torr range, while the pressure during deposition of the fluorides is below 6×10^{-7} Torr. The thicknesses and (optimized deposition temperatures) for the layers are 250 Å (200°C) for ZnF₂, 650 Å ($325\text{--}425^\circ\text{C}$) for MnF₂, $18\text{--}160 \text{ Å}$ (150°C) for Fe, and 50 Å (150°C) for Al. The Al overlayer is simply a cap material to prevent oxidation of the films, while ZnF₂ is a buffer layer to relax the large lattice mismatch (8%) between MgO and MnF₂. This is found to considerably improve the epitaxy. The growth of an Fe wedge is achieved with a moving shutter in close proximity to the substrate, driven by a vacuum stepper motor with $60 \mu\text{m}$ precision.

The layers have been characterized by reflection high-energy electron diffraction (RHEED), high-angle x-ray diffraction (HAXRD), in-plane x-ray diffraction, grazing incidence x-ray reflectivity (GIXR), and atomic force microscopy (AFM). We find that the fluoride layers are quasiepitaxial, twinned [110] films, while the metallic overlayers are polycrystalline with a [110] texture. The full width at half maximum (FWHM) of the high-angle [110] reflections of the AF fluoride layer is $\sim 2^\circ$ for every sample in this study. The interfacial roughness between the AF and F layers is controlled between 5 and 30 Å by varying the substrate temperature during growth.²¹ This interfacial roughness is a very important microstructural parameter as it defines the sign of the interfacial coupling between the F and AF layers and, as a consequence, whether the system exhibits positive exchange bias.^{12,21} The samples presented in this study were deliberately grown at temperatures, and interfacial roughnesses, which resulted in only negative exchange bias. This was done to allow a direct comparison with other simple systems where only negative exchange bias exists and the interfacial coupling is (presumably) ferromagnetic in nature.

Wedges were deposited onto 18-mm-wide substrates which were then cut into 0.5–1-mm slices for the magnetometry measurements. For an F layer thickness variation from 16 to 160 Å this results in a “slope” of 8 Å thickness variation per mm across the sample surface. We stress that the magnetometry was performed on cut samples rather than by scanning magneto-optical methods. The thickness of the layers was determined by GIXR with an absolute accuracy of the order of 10%. The magnetometry was done in a superconducting quantum interference device (SQUID) magnetometer between 10 and 300 K and in fields up to 2 kOe. The remnant fields in the superconducting solenoid were minimized by warming the magnet above its critical temperature and accounted for by measuring the apparent loop shift of unbiased single Fe thin films. In all cases the remnant fields were kept well below the exchange bias fields reported here. Anisotropic magnetoresistance (AMR) measurements were made with the field parallel to the dc current in a ^4He flow cryostat with a superconducting solenoid capable of stepping field in 0.7 Oe increments. Polarized neutron reflectometry

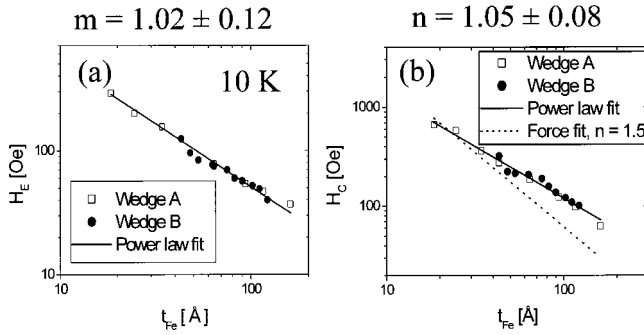


FIG. 2. $T = 10$ K Fe layer thickness dependence of the exchange bias (a) and coercivity (b) plotted on a log-log graph. Two wedges are shown (solid and open symbols). The solid lines are straight line fits which represent a power law as described by Eqs. (1) and (2). The dotted line in (b) is a force fit with $n = 1.5$ to illustrate that such a departure from $1/t_{Fe}$ would be easily resolvable in this experiment. $H_{FC} = 2$ kOe. $t_{AF} = 650$ Å.

(PNR) measurements were made on the NG1 reflectometer at the National Institute for Standards and Technology. Briefly, a polarized neutron beam is specularly reflected from a thin-film sample onto a polarization analyzer and detector. A total of four cross sections are measured: two non-spin-flip cross sections and two spin-flip cross sections (+− and −+). The spin-flip scattering intensity arises from a component of the sample magnetization vector perpendicular to the applied magnetic field which flips the neutron spin from up to down or vice versa. Hence the observation of a nonzero value for the spin-flip (SF) scatter is indicative of significant rotation of the magnetization, as this results in some component of the film magnetization being oriented perpendicular to the applied field direction. The measurements in this paper were made by saturating the film in one direction and then increasing the field in the opposite sense until the coercive point is reached. The intensity of the SF scatter then probes the relative importance of magnetization rotation and reverse domain nucleation and propagation.

RESULTS AND DISCUSSION

As expected, the films show exchange bias and enhanced coercivities with values typical for these growth conditions.²¹ As seen in previous studies,^{4–7,21} the blocking temperatures are identical to the bulk Néel temperature ($T_N = 67.3$ K) within experimental uncertainty. In addition, these samples were proven to give the same value for exchange bias energy regardless of whether the measuring technique is reversible or irreversible.²²

Figure 2 shows (on a log-log plot) the thickness dependence of the exchange bias and coercivity after field cooling from room temperature to 10 K in a field (H_{FC}) of 2 kOe. Note that two wedges are included on the plots (the open and solid symbols). These separate samples were fabricated on different “pump downs” of the vacuum system and the close agreement between the two is testament to the reproducibility we can achieve. The solid lines are straight line fits which represent a power-law dependence with a gradient equal to the power n for the coercivity and the power m for the ex-

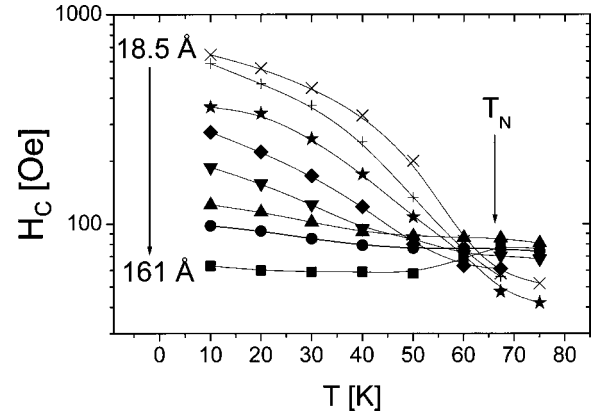


FIG. 3. Temperature dependence of the coercivity for one of the wedges shown in Fig. 2. The thicknesses of the Fe layer are 18.5, 24.5, 34, 43, 64, 93.5, 116, and 161 Å, respectively. The Néel point $T_N = 67.3$ K is labeled. $H_{FC} = 2$ kOe. $t_{AF} = 650$ Å.

change bias [see Eqs. (1) and (2)]. The fits result in values of $n = 1.02 \pm 0.12$ and $m = 1.05 \pm 0.08$, both consistent with $1/t_{Fe}$ dependences. Although the $1/t_{Fe}$ dependence is expected for the exchange bias (although small deviations are predicted in Ref. 15), for the coercivity it is in direct contradiction with the theoretical work of Li and Zhang¹⁴ and Stiles and McMichael¹⁵ as detailed in the Introduction. It is worth noting at this stage that a reduced temperature of $t = T/T_N = 10$ K/67.3 K is low enough to be in the low-temperature regime of the Stiles-McMichael model where a $1/t_{Fe}^2$ dependence is expected. The general arguments based on the Li-Zhang model predict $1/t_{Fe}^{1.5}$. In order to assess whether the present experiment is accurate enough to resolve such deviations from $1/t_{Fe}$ behavior, we have added a straight line with a gradient corresponding to the power $n = 1.5$ in Fig. 2. Clearly, this represents a resolvable departure from the dependence we observe.

The temperature dependence of the coercivity enhancement over the full range of Fe layer thickness is illustrated in Fig. 3 for a single wedge with thickness from 18.5 to 161 Å.²³ At low Fe thickness the coercivity is monotonically dependent on temperature, showing a sharp increase on cooling through T_N followed by a gradual saturation as $T \rightarrow 0$. However, at higher Fe thickness the temperature dependence is dominated by a broad maximum near T_N , in addition to a weak increase as $T \rightarrow 0$. These two regimes are delineated by a crossover thickness of ~ 90 Å (“up triangles” in Fig. 3) where the two contributions compete, resulting in a coercivity which is nearly temperature independent from 10 to 100 K.

It should be noted at this stage that broad peaks in the coercivity at the Néel point have been observed before, sporadically, in many systems.^{12,24–29} They also appear in some theoretical models, most notably the model of Stiles and McMichael.¹⁵ In general terms the existence of the peak at T_N is due to the losses in the AF layer as the Néel point is approached from below. The basic idea is that the fraction of total energy loss which occurs in the AF part of the AF/F bilayer is increasing as T_N is approached. As T_N is approached from below, the AF anisotropy is rapidly decreas-

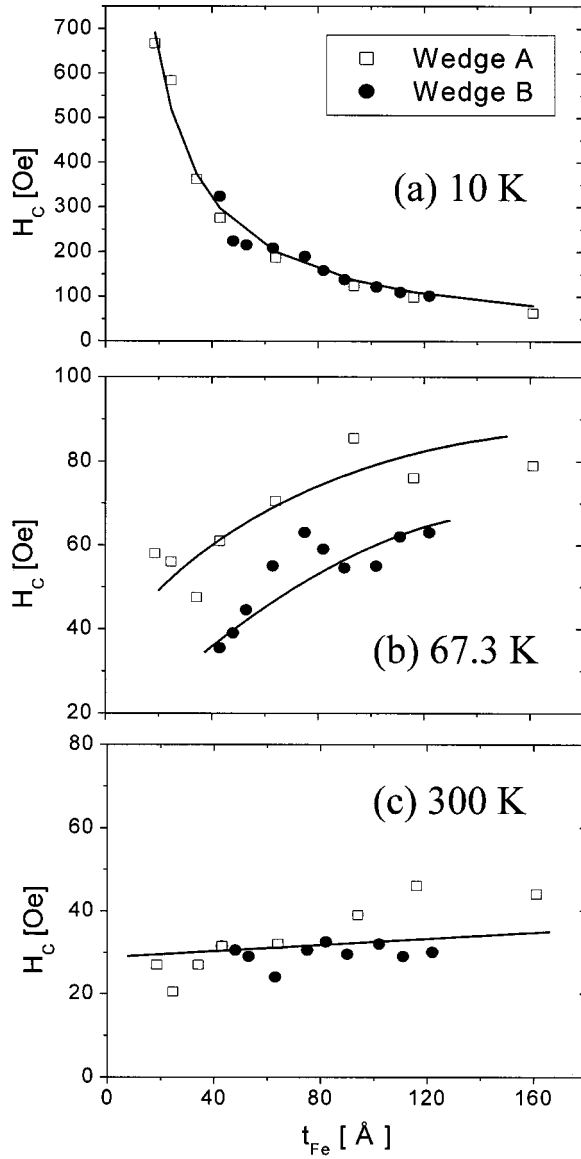


FIG. 4. Fe layer thickness dependence of the coercivity at (a) $T=10$ K, (b) $T=T_N=67.3$ K, and (c) $T=300$ K. In (a) the solid line is a $1/t_{Fe}$ fit, in (b) the solid line is a guide to the eye, and in (c) the solid line is a straight line fit. $H_{FC}=2$ kOe. $t_{AF}=650$ Å.

ing, meaning that reversal of the ferromagnet can induce more spin reorientation in the AF layer, and the coercivity increases. This continues until T_N where the AF order is lost and the effect is destroyed, meaning that the coercivity begins to decrease again, hence the broad peak roughly centered around T_N . Note that in the Stiles-McMichael model the energy losses in the AF layer are due to irreversible changes in spin structure, but the basic concept is similar.

The interesting point in our experiment is that these maxima in coercivity are only observed in thicker Fe layers. This phenomenon is illustrated again in Fig. 4, which shows the thickness dependences for the coercivity at three temperatures: 10 K, 67.3 K ($=T_N$), and 300 K. The 10 K data are already shown in Fig. 2 and show the previously discussed, strong $1/t_{Fe}$ dependence. The 67.3 K data actually show an *increase in coercivity with increasing thickness*, which is due

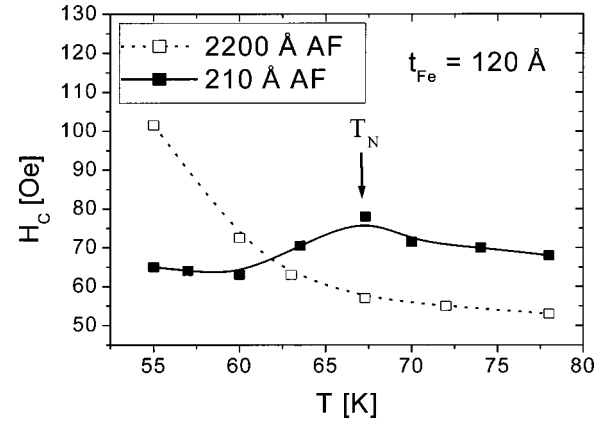


FIG. 5. Temperature dependence of the coercivity for two samples with $t_{Fe}=120$ Å and $t_{AF}=210$ Å (solid symbols) and $t_{AF}=2200$ Å (open symbols). $H_{FC}=2$ kOe.

to the fact that the broad maxima in H_C occur only for the thicker Fe layers. In other words, it appears that there are two components to the coercivity—one which is active at all temperatures, which is seen for all Fe thicknesses, and one which contributes only in the vicinity of T_N , which is only observed in thicker Fe layers. Upon increasing temperature to 300 K the coercivity becomes almost thickness independent as shown in Fig. 4(c). This is an interesting point in itself, to which we shall return later.

To gain insight into the origin of the H_C peak at T_N for larger Fe thicknesses we fabricated further samples with various AF layer thicknesses. The coercive behavior of these samples is summarized in Fig. 5, which shows $H_C(T)$ in the vicinity of T_N for a constant Fe layer thickness of 120 Å and AF layer thicknesses of 210 and 2200 Å, respectively. The sample with lower AF thickness shows a clear maximum in H_C at T_N , while the sample with large AF thickness shows no such maximum. The data suggest that the peak in H_C only occurs when the ratio of the F layer thickness to the AF layer thickness is bigger than a particular value; i.e., for a constant Fe layer thickness there is a peak for low AF thickness, but not for high AF thickness, as observed in Fig. 5.

To further test this hypothesis we fabricated three additional wedges of similar structure to that in Fig. 1, but with constant AF thicknesses of 220, 1000, and 2200 Å. Each of these wedges was subject to the same cutting procedure as the first wedge and was measured under identical conditions by SQUID magnetometry. Note also that the FWHM of the high-angle x-ray reflections and the interfacial roughnesses were comparable to those of the original two wedges shown in Fig. 2. In each case we observed that the peak at T_N occurs at large Fe thickness only. In fact, a crossover Fe thickness (t_{Fe}^*) delineates the two regimes, i.e., low thickness where the T dependence is monotonic and high thickness where it shows a broad maximum at T_N . Figure 6 shows the ratio t_{Fe}^*/t_{AF} plotted against t_{AF} , the thickness of the AF layer. Clearly the crossover between the two regimes always occurs at a specific value of the ratio of the F to AF layer thickness.

The two distinct regimes of coercive behavior may be due to the relative dominance of the F or AF layer, as suggested

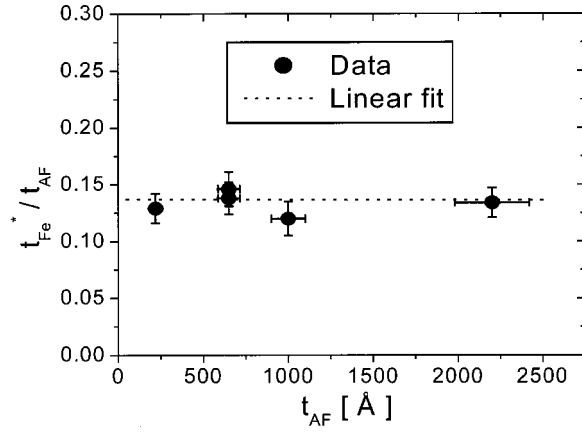


FIG. 6. Plot of the ratio of the crossover thickness t_{Fe}^* to the antiferromagnet thickness t_{AF} against the antiferromagnetic thickness for four wedges. The two wedges with AF thickness of 650 Å are the same as those studied in Figs. 2, 3, 4, and 5.

in the theoretical model of Stiles and McMichael.¹⁵ At low Fe thickness the losses on reversal of the F layer are primarily in the F layer itself and the temperature dependence of the coercivity is monotonic. At higher thicknesses we suggest that a significant fraction of the losses on reversal of the F layer take place in the AF layer. It is these losses which increase in importance as T_N is approached from below and lead to the maximum in $H_C(T)$. It is interesting to formulate this idea in terms of the relative strengths of the anisotropies in the F and AF layers. Denoting the AF and F anisotropy constants (in units of erg/cm³) as K_{AF} and K_F , the ratio of the anisotropy energies in the two layers is $X = K_F t_F / K_{\text{AF}} t_{\text{AF}}$. The argument above implies that when the F layer anisotropy energy is significant (i.e., when X is large, at high Fe layer thickness) the F layer induces significant spin reorientation in the AF layer as it reverses. On the other hand, when the F layer anisotropy energy is weak (i.e., when X is small, at low Fe layer thickness) the F layer reverses without perturbing the AF layer in the vicinity of T_N . Hence no anomaly is observed at T_N as the losses are primarily in the F layer itself. Although the proposed model is similar to that of Stiles and McMichael, we do not observe the predicted $1/t_{\text{Fe}}^2$ dependence, which could well be due to the fact that our system is, strictly speaking, outside the range of applicability of the Stiles-McMichael model.³⁰

At this stage we return to the observation of a high-temperature (300 K) coercivity which is essentially independent of the Fe layer thickness. In order to understand this effect we undertook an investigation of the nature of the reversal mechanism at low and high Fe thicknesses at 300 K, using PNR and AMR. Both of these techniques have been successfully employed in the past to probe the magnetization reversal in exchange-biased F layers.^{4–6,31,32} Previous measurements on similar samples with $t_{\text{Fe}} = 120$ Å indicated that the reversal mechanism at high temperatures was neither completely due to rotation of the magnetization nor completely due to domain wall nucleation and propagation.³³ The reversal mechanism appeared to be a mixture of the two as deduced from the fact that the intensity of the spin-flip scat-

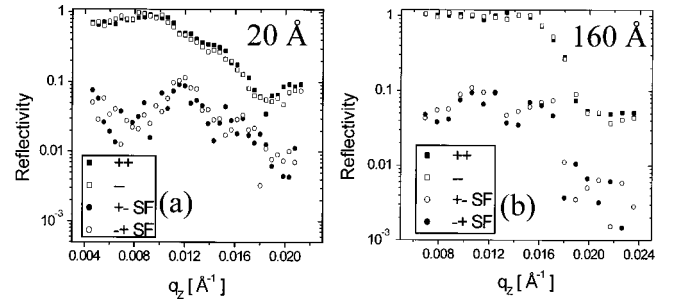


FIG. 7. Polarized neutron reflectivity against momentum transfer for two samples with $t_{\text{Fe}} = 20$ Å (a) and 160 Å (b), respectively. The data were taken after saturating the films in the negative field direction and then returning to a point close to the right-side coercive field. Square symbols represent non-spin-flip scattering, while the round symbols represent the spin-flip scattering intensity. In both cases, $T \gg T_N$.

tering at the coercive point (I_{SF}) in the PNR was far less than the full value expected for complete coherent rotation, but nonzero. This is a clear indication that the reversal is of mixed character with some domain wall contribution and some rotation of the magnetization.³⁴ Figure 7 shows the PNR at $T \gg T_N$ for samples with Fe thicknesses of 160 and 20 Å on a fixed 650-Å AF layer. These data were taken after saturating the F layers in the negative field direction and then returning to a point close to the coercive field on the right-hand side of the loops. Note that the data were corrected to take into account the finite spin polarization of the neutron beam and the background count rate. The overlap of the two non-spin-flip scattering profiles in each case is testament to the fact that the film is very close to the coercive point: i.e., the net magnetization projected on to the applied magnetic field vector is close to zero. The striking similarity of the two spin-flip data sets is in agreement with the fact that the H_C values barely differ (40 Oe compared to 50 Oe) despite the difference in F layer thickness and the completely disparate behavior at $T < T_N$ (see Fig. 3). Again, the nonzero values of I_{SF} suggest a significant amount of magnetization rotation. The AMR hysteresis loops for the two samples are shown in Fig. 8 at $T = 272$ K ($\gg T_N$), taken with the current perpendicular to the applied magnetic field direction. Again, the similarity is striking. Not only are the coercivity values and the general shape very similar, the amplitude of the AMR effect is practically identical (0.130% compared to 0.105%). Note that, just as for the PNR, the amplitude of the effect is consistent with a mixed reversal with both rotational and domain character.

We are led to the conclusion that the reversal mechanism and coercivity at 300 K is almost independent of the F layer thickness. This is inconsistent with reversal by domain wall motion as this will give a strong thickness dependence with higher H_C at low thickness values. Essentially, this is due to the fact that driving perpendicular domain walls through F layers become increasingly difficult as the thickness is reduced. We propose that the indications of significant magnetization rotation in the PNR and AMR data are the key to interpretation of the insensitivity of H_C to t_{Fe} . Specifically, we suggest that the F layer is composed of a large number of

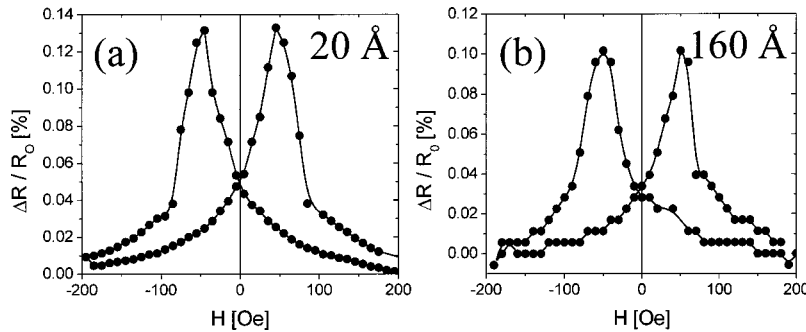


FIG. 8. Anisotropic magnetoresistance data for the two samples with $t_{\text{Fe}} = 20 \text{ \AA}$ (a) and 160 \AA (b), respectively. The data were taken at $T = 273 \text{ K}$ with the current aligned perpendicular to the in-plane magnetic field. In both cases the current used was 96 \mu A . The 20-\AA sample had a resistance of 65 \Omega , while the 120-\AA sample had a resistance of 4.5 \Omega (these values are at 273 K).

grains with a diameter which is largely independent of the thickness of the layer. The size of the coercivity is determined by the rotation of the magnetization in these individual grains and is therefore independent of the layer thickness. Ideally, we would be able to probe the microstructure of the F layers with our x-ray diffraction techniques, but this is impossible in this system due to the unfortunate overlap of the peak positions of the MgO [100] substrate reflection and the Fe [110] reflection. However, prior studies with AFM detected a surface morphology modulation, consistent with grains of the order of several hundred nanometers in diameter.

SUMMARY AND CONCLUSIONS

In summary, we have made a detailed investigation of the thickness dependence of the exchange bias and coercivity enhancement in well-characterized exchange-biased bilayers of Fe/MnF₂. At low temperatures we observe a $1/t_{\text{Fe}}$ dependence for both the exchange bias and coercivity, in apparent disagreement with recent theoretical predictions. The temperature dependence of the coercivity clearly implies the existence of two distinct regimes of coercive behavior. At large Fe layer thicknesses (or low antiferromagnet thickness) a broad maximum in the coercivity occurs near the Néel temperature. At low Fe layer thickness the temperature depen-

dence of the coercivity is monotonic. By varying the thickness of the AF layer we proved that the crossover point between the two regimes occurs at a well-defined ratio of the thickness of the F and AF layers. We propose that the two regimes correspond to situations where the F layer reverses almost independently of the AF layer near T_N (low Fe thickness) and where the F layer reversal induces significant loss in the AF layer (high Fe thickness). This is similar to a recent model by Stiles and McMichael.¹⁵

ACKNOWLEDGMENTS

We acknowledge illuminating discussions with K. Liu, B. J. Jönsson-Akerman, H. Suhl, J. Sivertsen, M. D. Stiles, and C. J. Palmström. B. J. Jönsson-Akerman is also thanked for his invaluable technical assistance with design of the wedge grower. The work at UCSD was supported by the U.S. DOE and the NSF, the work at Los Alamos was supported by the U.S. DOE BES-DMS under Contract No. W-7405-Eng-36, Grant No. DE-FG03-87ER-45332, and the UC CULAR, while the work at UofM was supported by the University of Minnesota Office of the Vice President For Research and Dean of the Graduate School. A.H. thanks the Los Alamos National Laboratory for support. We are grateful to the National Institute for Standards and Technology for the use of the neutron scattering facilities.

¹For recent reviews see J. Nogués and I. K. Schuller, *J. Magn. Mater.* **192**, 203 (1999); A. E. Berkowitz and K. Takano, *ibid.* **200**, 552 (1999).

²B. Dieny, V. S. Speriosu, S. S. P. Parkin, B. A. Gurney, D. R. Wilhoit, and D. Mauri, *Phys. Rev. B* **43**, 1297 (1997).

³V. I. Nikitenko, V. S. Gornakov, A. J. Shapiro, R. D. Shull, K. Liu, S. M. Zhou, and C. L. Chien, *Phys. Rev. Lett.* **84**, 765 (2000).

⁴M. R. Fitzsimmons, P. Yashar, C. Leighton, I. K. Schuller, J. Nogués, C. F. Majkrzak, and J. A. Dura, *Phys. Rev. Lett.* **84**, 3986 (2000).

⁵C. Leighton, M. Song, J. Nogués, M. C. Cyrille, and I. K. Schuller, *J. Appl. Phys.* **88**, 344 (2000).

⁶C. Leighton, M. R. Fitzsimmons, P. Yashar, A. Hoffmann, J. Nogués, J. Dura, C. F. Majkrzak, and I. K. Schuller, *Phys. Rev. Lett.* **86**, 4394 (2001).

⁷C. Leighton and I. K. Schuller, *Phys. Rev. B* (to be published).

⁸H. D. Chopra, D. X. Yang, P. J. Chen, H. J. Brown, L. J. Swartzendruber, and W. F. Egelhoff, Jr., *Phys. Rev. B* **61**, 15 312 (2000).

⁹X. Portier, A. K. Petford-Long, A. de Morais, N. W. Owen, H. Laidler, and K. O'Grady, *J. Appl. Phys.* **87**, 6412 (2000).

¹⁰W.-T. Lee, S. G. E. te Velthuis, G. P. Felcher, F. Klose, T. Gredig, and E. D. Dahlberg (unpublished).

¹¹T. C. Schulthess and W. H. Butler, *Phys. Rev. Lett.* **81**, 4516 (1998).

¹²C. Leighton, J. Nogués, B. J. Jönsson-Akerman, and I. K. Schuller, *Phys. Rev. Lett.* **84**, 3466 (2000).

¹³Y. J. Tang, B. Roos, T. Mewes, S. O. Demokritov, B. Hillebrands, and Y. J. Wang, *Appl. Phys. Lett.* **75**, 707 (1999).

¹⁴Z. Li and S. Zhang, *Phys. Rev. B* **61**, R14 897 (2000).

¹⁵M. D. Stiles and R. D. McMichael, *Phys. Rev. B* **63**, 064405 (2001); **60**, 12 950 (1999); **59**, 3722 (1999).

¹⁶P. Miltenyi, M. Gierlings, J. Keller, B. Beschoten, G. Güntherodt,

- U. Nowak, and K. D. Usadel, *Phys. Rev. Lett.* **84**, 4224 (2000).
- ¹⁷T. Gredig, I. N. Krivorotov, C. Merton, A. M. Goldman, and E. D. Dahlberg, *J. Appl. Phys.* **87**, 6418 (2000).
- ¹⁸D. V. Dimitrov, S. Zhang, J. Q. Xiao, G. C. Hadjipanayis, and C. Prados, *Phys. Rev. B* **58**, 2090 (1998).
- ¹⁹S. Zhang, D. V. Dimitrov, G. C. Hadjipanayis, J. W. Cai, and C. L. Chien, *J. Magn. Magn. Mater.* **198–199**, 468 (1999).
- ²⁰S. M. Zhuo, K. Liu, and C. L. Chien, *J. Appl. Phys.* **87**, 6659 (2000).
- ²¹C. Leighton, J. Nogués, H. Suhl, and I. K. Schuller, *Phys. Rev. B* **60**, 12 837 (1999).
- ²²E. D. Dahlberg, B. Miller, B. Hill, B. J. Jönsson-Åkerman, V. Ström, K. V. Rao, J. Nogués, and I. K. Schuller, *J. Appl. Phys.* **83**, 6893 (1998).
- ²³Note that the data displayed in this figure are from the exact same wedge as studied in Fig. 2.
- ²⁴C. Hou, H. Fujiwara, K. Zhang, A. Tanaka, and Y. Shimizu, *Phys. Rev. B* **63**, 024411 (2001).
- ²⁵S. Poppe, H. Nembach, A. Mougin, T. Mewes, J. Fassbender, and B. Hillebrands (unpublished).
- ²⁶F. B. Hagedorn, *J. Appl. Phys.* **38**, 3641 (1967).
- ²⁷S. H. Charap and E. Fulcomer, *J. Appl. Phys.* **42**, 1426 (1971).
- ²⁸P. A. A. van der Heijden, T. F. M. M. Mass, W. J. M. de Jonge, J. C. S. Kools, F. Roozeboom, and P. J. van der Zaag, *Appl. Phys. Lett.* **72**, 492 (1998).
- ²⁹J. Nogués and I. K. Schuller, *J. Magn. Magn. Mater.* **192**, 203 (1999)—see p. 224, Fig. 13.
- ³⁰Their model is specifically for the situation where the AF and F layers are polycrystalline, although the twin boundaries in our sample may play a similar role to the grain boundaries in polycrystalline systems. Moreover, this model may not be applicable when the system is susceptible to formation of ferromagnetic domain walls parallel to the interface as demonstrated for fluorides by M. Kiwi, J. Mejía-Lopez, R. D. Portugal, and R. Ramirez, *Europhys. Lett.* **48**, 573 (1999).
- ³¹A. R. Ball, A. J. G. Leenaers, P. J. van der Zaag, K. A. Shaw, B. Singer, D. M. Lind, H. Frederikze, and M. T. Rekveldt, *Appl. Phys. Lett.* **69**, 1489 (1996); Y. Ijiri, J. A. Borchers, R. W. Irwin, S.-H. Lee, P. J. van der Zaag, and R. M. Wolf, *Phys. Rev. Lett.* **80**, 608 (1998).
- ³²W.-T. Lee, S. G. E. te Velthuis, G. P. Felcher, F. Klose, T. Gredig, and E. D. Dahlberg (unpublished); S. G. E. te Velthuis, A. Berger, G. P. Felcher, B. K. Hill, and E. D. Dahlberg, *J. Appl. Phys.* **87**, 5046 (2000); S. G. E. te Velthuis, J. S. Jiang, and G. P. Felcher, *Appl. Phys. Lett.* **77**, 2222 (2000).
- ³³M. R. Fitzsimmons, C. Leighton, A. Hoffmann, P. C. Yashar, J. Nogués, I. K. Schuller, K. Liu, C. F. Majkrzak, J. A. Dura, and H. Fritzsche, *Phys. Rev. B* (to be published).
- ³⁴The exact fraction of film moment which is oriented perpendicular to the applied field direction can be extracted by simple modeling (see Ref. 31).